

The COBE Normalization of CMB Anisotropies

Martin White and Emory F. Bunn

*Center for Particle Astrophysics, University of California,
Berkeley, CA 94720-7304*

ABSTRACT

With the advent of the COBE detection of fluctuations in the Cosmic Microwave Background radiation, the study of inhomogeneous cosmology has entered a new phase. It is now possible to accurately normalize fluctuations on the largest observable scales, in the linear regime. In this paper we present a model-independent method of normalizing theories to the full COBE data. This technique allows an extremely wide range of theories to be accurately normalized to COBE in a very simple and fast way. We give the best fitting normalization and relative peak likelihoods for a range of spectral shapes, and discuss the normalization for several popular theories. Additionally we present both Bayesian and frequentist measures of the goodness of fit of a representative range of theories to the COBE data.

Subject headings: cosmic microwave background – methods: statistical

Introduction

Classically, it has been standard practice to normalize models of large-scale structure at a scale of $\simeq 10 h^{-1}\text{Mpc}$, using a quantity related to the clustering of galaxies (here the Hubble constant $H_0 = 100 h \text{ km s}^{-1} \text{ Mpc}^{-1}$) measured at the current epoch. Due to processing of the primordial spectrum and the large amplitude of the mass fluctuations which galaxies represent, this method of normalization requires assumptions about the history of the equation of state for matter inside the horizon, the non-linear evolution of the density field and the processes of galaxy formation. One of the key uncertainties is the relationship between the observed structure and the underlying mass distribution in the universe. With the COBE DMR detection of Cosmic Microwave Background (CMB) anisotropies (Smoot et al. 1992), it has become possible to directly normalize the potential fluctuations at near-horizon scales, circumventing the problems with the ‘conventional’ normalization.

In an earlier *Letter* we presented the normalization of the standard cold dark matter (CDM) model and a small range of variants (Bunn, Scott & White 1995). In this paper we extend this to a larger class of models, and present a means for normalizing a whole class of models to the COBE data in a computationally simple manner. Throughout we will use the 2-year COBE data (Bennett et al. 1994, Górski et al. 1994, Wright et al. 1994, Banday et al. 1994, Górski et al. 1995a) as released by NASA–GSFC. The normalization in this data differs from that in the data used by the COBE group by $\sim 1\mu\text{K}$ (K.M. Górski, private communication; Górski et al., 1995b).

As discussed in Bunn et al. (1995) and Banday et al. (1994) there is more information in the COBE data than just the RMS power measured. In other words, the COBE data cannot be reduced to a single number without a significant loss of information. One way to see this is to notice that there are ~ 90 eigenvalues of the signal-to-noise ratio with eigenvalue larger than 1. An alternative method is to note that the COBE data constrains the amplitude of the fluctuations over a range of scales, albeit a narrow range.

In Fig. 1 we show the RMS power in a model which is fitted to the COBE data with one free parameter. The toy model we have chosen is the so called Sachs-Wolfe spectrum (Sachs & Wolfe 1967) which assumes that the observed temperature fluctuations come purely from the redshifts associated with climbing out of potentials on the last scattering surface (for a discussion see e.g. Peebles 1993; White, Scott & Silk 1994). Aside from the normalization of the model (which is fixed by COBE) there is one free parameter: the spectral slope, denoted n , with $n = 1$ corresponding to a scale invariant spectrum. We notice that the total power is not constant, showing that the normalization to COBE is sensitive to more than the total RMS fluctuations produced. Furthermore, the COBE data contain information on the “shape” of the power spectrum, which means that some theories are more likely than others, given the data. We will now introduce a simple method for using all of the information in the COBE data to normalize a wide class of models.

Model independent analysis

We have demonstrated that the COBE data contain more information than just the total power, which can be measured by $\langle Q \rangle$, $\sigma(10^\circ)$, $\sigma(7^\circ)$, band power, etc. However, it is still useful to have a method for normalizing a given model to the data, without having to use the full sky maps containing 6144 pixels at 3 frequencies in each of two channels. We present here a method which allows one to normalize a large class of theories (those which can be described by a power spectrum over the limited range of scales probed by COBE) to the data in a simple manner.

To proceed we notice that theories with gaussian fluctuations (or fluctuations which are gaussian on COBE scales) can be specified entirely in terms of a power spectrum. In CMB studies this is usually expressed as the variance of the multipole moments, as a function of mode number, i.e. $\ell(\ell + 1)C_\ell$ vs ℓ , where the temperature on the sky has been expanded in spherical harmonics

$$\frac{\Delta T}{T}(\theta, \phi) \equiv \sum_{\ell m} a_{\ell m} Y_{\ell m}(\theta, \phi) \quad (1)$$

and we define

$$\langle a_{\ell m}^* a_{\ell' m'} \rangle \equiv C_\ell \delta_{\ell\ell'} \delta_{mm'} \quad (2)$$

For most theories the power spectrum is a smooth function. Following White (1994), we will write

$$D(x) = \ell(\ell + 1)C_\ell \quad \text{with } x = \log_{10} \ell \quad (3)$$

We can perform a Taylor series expansion of $D(x)$ about some fiducial point, which we shall take to be $x = 1$ ($\ell = 10$). Many theories (see below) can be well approximated

by quadratic $D(x)$ over the relevant range for COBE, roughly $\ell = 2$ to 30, and so we present the normalizations and likelihoods of quadratic $D(x)$. We choose to parameterize our quadratics by the (normalized) first and second derivatives at $x = 1$: D'_1 and D''_1 where

$$D(x) \simeq D_1 \left(1 + D'_1(x-1) + \frac{D''_1}{2}(x-1)^2 \right) \quad (4)$$

(note that D'_1 is $1/D_1$ times the derivative of $D(x)$ at $x = 1$). The normalization is then given by quoting D_1 , or C_{10} , for each (D'_1, D''_1) pair, and the goodness of fit is quantified by the relative likelihood of that shape compared to a featureless, $n = 1$, Sachs-Wolfe spectrum.

We compute the maximum-likelihood normalization for a grid of values of D'_1 and D''_1 using the method described in Bunn & Sugiyama (1995) and Bunn et al. (1995). We combine the six publicly-available equatorial DMR sky maps pixel by pixel into a single map by performing a weighted average, with weights given by the inverse square of the noise level in each pixel. (We obtain negligibly different results when the two 31 GHz maps, which are more sensitive to Galactic contamination, are excluded. These maps have high noise levels, and are therefore automatically given low weights in the average.) We excise all pixels whose centers have Galactic latitude $|b| < 20^\circ$ from the map, leaving 4038 pixels.

We then estimate the likelihood of getting this particular data set for each power spectrum. Rather than computing the likelihood directly, which would involve repeated inversions of a 4038×4038 matrix, we first perform a Karhunen-Loève transform (Karhunen 1947, Thierren 1992) to “compress” the data to a more manageable size. Specifically, we choose a set of basis functions f_i defined on the portion of the sphere outside of the Galactic cut. (The manner in which these functions are chosen is described below.) We then compute the inner product of the data vector with each of these functions:

$$x_i = \sum_j f_i(\hat{\mathbf{r}}_j) \Delta T(\hat{\mathbf{r}}_j), \quad (5)$$

where $\hat{\mathbf{r}}_j$ is the position of the j th pixel, $\Delta T(\hat{\mathbf{r}}_j)$ is the corresponding temperature fluctuation in the data, and the sum runs over all pixels. If we assume that the temperature fluctuations are gaussian, then the projections x_i will be gaussian as well. We can therefore compute their likelihood in the usual way:

$$L \propto (\det V)^{-1/2} \exp \left(-\frac{1}{2} x_i V_{ij}^{-1} x_j \right), \quad (6)$$

where $V_{ij} \equiv \langle x_i x_j \rangle$ is the covariance matrix, which contains contributions from the cosmic signal and the noise:

$$V = V_{\text{sig}} + V_{\text{noise}} = (FY)(BCB)(FY)^T + FNF^T, \quad (7)$$

where $F_{ij} = f_i(\hat{\mathbf{r}}_j)$, $Y_{i\mu} = Y_{\ell m}(\hat{\mathbf{r}}_i)$, $C_{\mu\nu} = C_\ell \delta_{\mu\nu}$, B is the beam pattern, and $N_{ij} \approx \sigma_i^2 \delta_{ij}$ is the covariance matrix of the noise in the sky map. (Here Greek indices stand for pairs of indices (ℓm) , with $\mu = \ell^2 + \ell + m + 1$.)

The Karhunen-Loève transform is a prescription for choosing the basis functions f_i , or equivalently the elements of the matrix F . We choose the functions so that the likelihood in eq. (6) will have maximal rejection power for incorrect models. We therefore want the likelihood L to be, on average, as sharply peaked as possible about its maximum, or in other words, we want to choose F_{ij} to maximize $\langle -L'' \rangle$, where the primes denote derivatives with respect to some parameter in our theoretical model and the derivatives are evaluated at the maximum of L . This optimization problem reduces to a generalized eigenvalue problem: each row f_i of F satisfies the equation

$$V_{\text{sig}} \vec{f} = \lambda V_{\text{noise}} \vec{f}. \quad (8)$$

Furthermore, the rows should be chosen to have the maximum eigenvalues λ . Rows with small values of λ probe mostly the distribution of the noise, with little sensitivity to the cosmological signal. They can therefore be omitted from the likelihood estimates with little loss of information. We have found that it is necessary to keep only the 400 most significant modes.

Since we have no knowledge of the true monopole and dipole in the sky map, we marginalize over these modes. The peak value, width and location of this final marginalized likelihood, as a function of D_1 , D'_1 and D''_1 , are the output of the fitting procedure.

Now to find the normalization of any theory, one calculates the large-angle multipole moments and finds the quadratic which best describes their shape. Over the range $-0.5 \leq D'_1 \leq 0.5$ and $-0.5 \leq D''_1 \leq 3.5$, the best-fitting amplitude and likelihood are given by the following analytic forms:

$$10^{11} C_{10} = 0.8073 + 0.0395 D'_1 - 0.0193 D''_1 \quad (9a)$$

$$\ln L = 0.00697 + 1.523 D'_1 - 0.403 D_1'^2 - 0.490 D''_1 - 0.0391 D'_1 D''_1 + 0.00855 D_1''^2 \quad (9b)$$

The fitting formula for C_{10} has a worst-case error of 2% and an average error of 0.4% over this range; the corresponding numbers for L (not $\ln L$) are 7% and 1.7%. The uncertainty in C_{10} is approximately 15% for all models. Note that the COBE data prefer models with positive D'_1 and negative D''_1 . The likelihood reaches its maximum at the point $(D'_1, D''_1) = (0.0, -3.0)$, which is beyond the range covered by the fitting formula. The peak likelihood for this model is 3.7 times the likelihood of a flat Harrison-Zel'dovich model. Fig. 2 shows L as a function of D'_1 and D''_1 .

In Tables 1 and 2 we show the best fitting shape parameters for some flat, low- Ω_0 variants of the CDM model. The fit of a quadratic to these theories gives an error at the worst fit multipole (in the range $\ell = 2$ to 30) of about 5%, with a typical error of $\lesssim 2\%$, showing that such theories are well fit by quadratics over the range of scales probed by COBE. To quantify the error introduced by approximating the power spectrum as a quadratic, we computed likelihood curves for the *worst*-fitting model in our sample using both the true power spectrum and the quadratic approximation. The two curves differ by 11% in peak likelihood and by 0.5% in normalization.

Critical ($\Omega_0 = 1$) CDM models with late reionization are also well fit by quadratic $D(x)$. The most plausible, though not the only, ionization history in hierarchical models

of structure formation is standard recombination, followed by full ionization from some redshift z_* until the present. The fully ionized phase is due (perhaps) to radiation from massive stars on scales which go non-linear early. (See Liddle & Lyth 1995 for further discussion.) We find that, over the range of ℓ probed by COBE, models which have $z_* \lesssim 100$ are almost indistinguishable from models with no reionization, assuming standard big-bang nucleosynthesis values for Ω_B . There is of course damping on degree scales ($\ell \sim 100$), but little change in the spectrum at smaller ℓ . Further, the relative normalization of the matter and radiation power spectra is the same as in models with standard recombination. For a CDM model with $h = 0.5$ and $n = 1$, the quadratic parameters are well fit by the formulae

$$\begin{aligned} D'_1 &= 0.738 - 0.0307z_* + 3.32 \times 10^{-4}z_*^2 - 1.06 \times 10^{-6}z_*^3 \\ D''_1 &= 1.554 - 0.0483z_* + 3.67 \times 10^{-4}z_*^2 - 7.60 \times 10^{-7}z_*^3 \end{aligned} \quad (10)$$

over the range $30 \leq z_* \leq 110$.

The case of open CDM models is more complicated, since the C_ℓ exhibit features at several scales. To add to the difficulty, there appear to be several different primordial spectra one can consider in open universe models. Some models based on inflationary phases (Lyth & Stewart 1990, Ratra & Peebles 1994, Bucher, et al. 1995) predict power spectra which show an increase in power near the curvature radius. All of these calculations make use of basis functions in which there is exponential damping of power above the curvature radius; however, this assumption can be relaxed (Lyth & Woszczyna 1995, Yamamoto et al. 1995). For further discussion of these issues see the appendix. The open models of Ratra & Peebles (1994) have already been fitted to the 2-year COBE data (Górski et al. 1995a) and we will not duplicate the results here. We mention, however, that the C_ℓ for such models can be fitted by cubics in $\log_{10} \ell$ to the same accuracy that the Λ CDM models can be fitted by quadratics. This increases the dimension of the parameter space and makes tabulating the results more difficult. We defer consideration of cubic fits until the situation with regard to open models is more settled.

Once the 4-year COBE data becomes available, we hope a fitting formula similar to Eq. 9 (but which goes to sufficiently high order to encompass almost all theories), could be produced for the benefit of the astrophysics community. Such a fit, coded into a subroutine, would allow any theory to be quickly and accurately fitted to the COBE data. At present our simple quadratic fit is sufficient for a wide range of theories of current interest.

The goodness of fit

Statistical methods for using a data set like COBE to place constraints on models generally come in two varieties, Bayesian and frequentist. Most CMB work, including analyses of the COBE data as well as other experiments, has taken a Bayesian point of view. In the Bayesian approach, the probability of observing the actual data is computed for each model. This may be denoted $p(D|M)$, meaning “the probability of the data given the model”. One then assumes a “prior” probability distribution $p(M)$ on the models and applies Bayes’s theorem to produce a “posterior” probability distribution giving the likelihood $p(M|D)$ of the various models given the data:

$$p(M|D) \propto p(D|M)p(M). \quad (11)$$

The posterior probability distribution tells us how likely each member of our family of models is compared with any other member, which is what we would like to know.

The Bayesian approach is perfectly adequate for assessing the *relative* merits of the various models under consideration: with this approach we can say, for example, that model A is 10 times more likely than model B. These models may only differ by a normalization or could be drawn from different cosmologies or structure formation scenarios. In some cases however we would like to assign *absolute* consistency probabilities to models. The Bayesian approach is not well suited to answering this sort of question, and the problem of assigning an absolute consistency probability to a model is best attacked with frequentist methods.

In the frequentist approach, we choose some goodness-of-fit parameter η , and compute its probability distribution over a hypothetical ensemble of realizations of the model. We then compute the value of η corresponding to the real data, and determine the probability of finding a value of η as extreme as the observed value in a random member of our ensemble. We take this probability to be a measure of the consistency of the data with the model: if the data does not occur often in realizations of the model, we say the model is “unlikely” given the data.

Two points about this technique deserve emphasis. First, the consistency probabilities derived in this manner are conceptually quite distinct from Bayesian likelihoods. Bayesians and frequentists ask different questions of their data, and will therefore sometimes get different answers. We do expect that models which have low Bayesian likelihoods will in general have poor frequentist consistency probabilities; however, there is no generally applicable quantitative relation between the two. Second, it is clear that the success of the frequentist approach depends on choosing an appropriate goodness-of-fit parameter η . For some classes of problems a standard choice is available; for the problem we consider below, we are unaware of such a standard. This is because the measurement of CMB fluctuations involves detecting extra noise on the sky. Thus the correlation function, or errors on the temperatures, which are used in the fit depend on the theory being tested, unlike normally examined cases of model fitting.

We wish to assign frequentist consistency probabilities to various power spectra. The first goodness-of-fit parameter one might think of for this purpose is a simple χ^2 ,

$$\chi^2 \equiv \sum_{i=1}^M \left(\frac{x_i}{\sigma_i} \right)^2, \quad (12)$$

where x_i is the amplitude of the i th element in our eigenmode expansion, σ_i^2 is the variance predicted for x_i by our model, and M is the number of modes in the expansion. (In order to remove all sensitivity to the monopole and dipole, the eigenmodes f_i should be orthogonalized with respect to these modes before the x_i are computed.) This parameter would be a natural choice if we wished to constrain the normalization of a model; however, our primary interest is in constraining the *shape* of the power spectrum, and this goodness-of-fit parameter is not well suited for this purpose. In fact, given *any* power spectrum C_ℓ , we can choose a normalization that gives a χ^2 that lies exactly at the median of its

probability distribution, since σ_i scales with the normalization of the theory. We would therefore conclude that for some normalization this model is a perfectly good fit regardless of the shape of the C_ℓ .

To focus on the power spectrum, let us consider quantities quadratic in the amplitude of the eigenmodes. There is a complication due to the presence of the galaxy in the COBE maps, which breaks the rotational symmetry of the COBE sky. This makes it difficult to define a rotationally symmetric quantity (like C_ℓ) by summing over azimuthal variable m . However, this is only a technical complication and we can still define a measure of power by binning the squares of the mode amplitudes in bins that probe particular angular scales. We expand each eigenmode f_i in spherical harmonics and compute an “effective ℓ ” probed by that mode by performing a weighted average over ℓ with weights given by the squares of the coefficients of the expansion. (The modes are generally quite narrow in ℓ -space, so the results are not sensitive to the exact method of computing the effective ℓ .) We then sort the modes in order of increasing effective ℓ (decreasing angular scale). As it happens, the result of this procedure is almost identical to sorting the modes in order of decreasing signal-to-noise eigenvalue. We then compute the quantities

$$z_i = \sum_{j=(i-1)K+1}^{iK} \left(\frac{x_j}{\sigma_j} \right)^2 \quad (13)$$

for $1 \leq i \leq M/K$. We should choose the bin size K to be large enough to reduce the intrinsic width of the distribution of z_i to a reasonable level, yet small enough that the mode amplitudes in each bin probe similar angular scales. We have adopted $K = 10$ as a compromise between these two considerations.

If our model is correct, then each z_i will be approximately K . If the model is incorrect, then some z_i will be too low, and others will be too high. For example, if our model has too little large-scale power, then the variances x_j/σ_j will be greater than 1 for small j , and the first few z_i will tend to be larger than K . We can quantify this observation by defining the goodness-of-fit parameter

$$\eta = \sum_{i=1}^{M/K} (z_i - K)^2. \quad (14)$$

The z_i for a Harrison-Zel’dovich spectrum and our worst-fitting model (model 4 of Table 3) are shown in Fig. 3. (In making Fig. 3 we chose the coarser bin size $K = 20$ rather than $K = 10$, to reduce scatter in the points.) Note that with our definition the z_i only loosely correspond to C_ℓ and depend on the theory. When z_i is larger than its expected value, one can conclude that the data have more power than the theory on the corresponding angular scale; however, there is *no* direct proportionality between z_i and the corresponding C_ℓ . Each z_i can be regarded as an estimator of the power spectrum of the signal and noise *combined*. For small i , z_i samples mostly signal, while the noise dominates for large i . The value of z_i for large i therefore changes very little as the model parameters are varied, as can be seen in Fig. 3.

Since the mode amplitudes x_i are in general correlated, it is not possible to compute analytically the probability distribution of η . We must therefore resort to Monte Carlo simulations. For each of several models, we created 1,000 random sky maps. We added noise to each pixel by choosing independent gaussian random numbers with zero mean and standard deviations corresponding to the noise levels in the real data. We computed the parameter η for each map. We chose to simulate six different models. The first four were chosen to span a range of values of the Bayesian likelihood: we simulated (1) a Harrison-Zel'dovich spectrum; the models with the (2) highest and (3) lowest Bayesian likelihoods from our grid of quadratic power spectra; and (4) a model with an even lower Bayesian likelihood $L = 0.01L_{HZ}$. In addition, we chose two models from Table 1 which have identical cosmological parameters ($\Omega_0 = 0.1$, $h = 0.75$, $n = 0.85$), except that (5) one has only scalar perturbations and one (6) includes tensors in the ratio $C_2^T/C_2^S = 7(1-n)$.

Our simulation procedure fails to mimic the real COBE data in at least two ways. First, the assumption that the noise in different pixels is independent is not strictly true (Lineweaver et al. 1994). However, the correlations are quite weak and have been shown to have negligible effects in analyses similar to ours (Tegmark & Bunn 1995). Second, we have not attempted to model the removal of systematic effects from the data. However, we expect this to have little effect on the final results, since the removal of systematic effects primarily affects the low- ℓ multipoles, while proper treatment of the noise is more important for the high values of ℓ where noise dominates.

It is clear from Table 3 that low Bayesian likelihoods tend to correspond to poor frequentist consistency probabilities, as expected. Furthermore, those models with likelihoods of order unity are reasonable fits to the data. This is a very reassuring fact: it was perfectly possible *a priori* that all the models we have been considering would prove to be intrinsically poor fits to the data. Comparison with the consistency probabilities for models 5 and 6 and a look at Fig. 4 allows one to calibrate the sensitivity of the COBE data to spectral shape information. We expect this to improve with the 4-year data, especially at higher ℓ .

The matter power spectrum

The best normalization and the goodness of fit of the temperature fluctuations for a range of models are given by Eq. 9. Using these results to normalize the matter power spectrum from the CMB can present some complications. In the simplest picture, in which large-angle CMB anisotropies come purely from potential fluctuations on the last scattering surface, the relative normalization of the CMB and matter power spectrum today is straightforward (White, Scott & Silk 1994, Bunn et al. 1995). In the conventional notation where the radiation power spectrum is given by

$$C_\ell = C_2 \frac{\Gamma(\ell + \frac{n-1}{2}) \Gamma(2 + \frac{5-n}{2})}{\Gamma(2 + \frac{n-1}{2}) \Gamma(\ell + \frac{5-n}{2})}. \quad (15)$$

the matter power spectrum for an $\Omega_0 = n = 1$ CDM universe is

$$\begin{aligned} P(k) &= 2\pi^2 \eta_0^4 A k T_m^2(k) \\ &\simeq 2.5 \times 10^{16} A (k/h \text{ Mpc}^{-1}) T^2(k) \quad (h \text{ Mpc}^{-1})^3. \end{aligned} \quad (16)$$

with $A = 3C_2/(4\pi)$. In models such as CDM this relation works quite well, as long as matter-radiation equality is sufficiently early (h is not too low). Even for $h = 0.3$ the relation works at the 4% level and if $h = 1$ the error is $\lesssim 1\%$. See Bunn et al. (1995) for further discussion.

For models with $\Omega_0 < 1$ the normalization is not so straightforward. Naively one would think that, for fixed CMB fluctuations at $z = 1,000$, one would have smaller matter fluctuations today. This is because in an open or a flat model with a cosmological constant ($\Omega_\Lambda = 1 - \Omega_0$), density perturbations stop growing once either the universe becomes curvature or cosmological constant dominated (respectively). Curvature domination occurs quite early, and the growth of density fluctuations $\delta\rho/\rho \equiv \delta$ in an open universe is suppressed (relative to an $\Omega_0 = 1$ universe) by a factor $\Omega_0^{0.6}$. In a flat Λ model, the cosmological constant dominates only at late times and so the growth suppression is a weaker function of the matter content: $\delta \propto \Omega_0^{0.23}$. This suppression of growth in an $\Omega_0 < 1$ universe has often been cited as “evidence” that Ω_0 must be large — otherwise fluctuations could not have grown enough to form the structures we observe today.

In fact there are several other effects which come into play when normalizing the matter power spectrum to the COBE data in a low- Ω_0 model. The first is that, though the growth in such models is suppressed by Ω_0^p ($p \simeq 0.6$ for open and 0.23 for Λ models; for a more general formula see Carroll et al. 1992), the potential fluctuations are proportional to Ω_0 . Hence the CMB fluctuations are even more suppressed than are the density fluctuations! So for a fixed COBE normalization the matter fluctuations today are *larger* in a low- Ω_0 universe, and the cosmological constant model clearly has the most enhancement since the fluctuation growth is the least suppressed. In terms of the power spectrum, $P(k)$, we expect for fixed COBE normalization that $P(k) \propto \delta^2 \propto \Omega_0^{2(p-1)}$, as has been pointed out by Efstathiou, Bond & White (1992).

This potential suppression is not the only effect which occurs in low- Ω_0 universes, although it is the largest. Due to the fact that the fluctuations stop growing (or in other words the potentials decay) at some epoch, there is another contribution to the large-angle CMB anisotropy measured by COBE. In addition to the redshift experienced while climbing out of potential wells on the last scattering surface, photons experience a cumulative energy change due to the decaying potentials as they travel to the observer. If the potentials are decaying, the blueshift of a photon falling into a potential well is not entirely canceled by a redshift when it climbs out. This leads to a net energy change, which accumulates along the photon path. This is often called the Integrated Sachs-Wolfe (ISW) effect, to distinguish it from the more commonly considered redshifting which has become known as the Sachs-Wolfe effect (both effects were considered in the paper of Sachs & Wolfe 1967). This ISW effect will operate most strongly on scales where the change of the potential is large over a wavelength, so preferentially on large angles (Kofman & Starobinsky 1985).

In Λ models the ISW effect can change the relative normalization of the matter and radiation fluctuations at the 25% level for $\Omega_0 \sim 0.3$ (see below). We show in Fig. 5 how these various effects on the inferred matter power spectrum normalization scale with Ω_0 in a cosmological constant universe (the simplest case). We see the total power is slightly changed, for fixed C_{10} , because the shape of the C_ℓ depend on Ω_0 . This affects the goodness

of fit with the COBE data (see Bunn & Sugiyama 1995 and our Eq. 9b). The ratio of the large-scale matter normalization to C_{10} is changed by the ISW contribution to C_{10} , the change in the potentials and the growth of fluctuations from $z = 1,000$ to the present. Over the range $\Omega_0 = 0.1$ to 0.5 one finds for an $n = 1$ spectrum with $C_{10} = 10^{-11}$

$$\lim_{k \rightarrow 0} \frac{P(k)}{k} = 1.14 \times 10^6 \Omega_0^{-1.35} \quad (h^{-1} \text{Mpc})^4 \quad (17)$$

almost independent of h . This can be compared with the scaling presented above. Also the epoch of matter-radiation equality is shifted, which changes the normalization on smaller scales for fixed large-scale $P(k)$. Putting these effects together we show the RMS fluctuation on a scale $0.028 h \text{Mpc}^{-1}$ (see below) as a function of Ω_0 in Fig. 6. The sharp downturn at low Ω_0 is due to a combination of the larger scale of matter-radiation equality, moving the break in the power spectrum to smaller k , and the photon drag on the baryons having an increased effect on fluctuation growth for large Ω_B/Ω_0 . For $\Omega_0 \simeq 0.3$ the shift in matter-radiation equality and the scaling of Eq. (17) roughly cancel, making Δ^2 much less sensitive to Ω_0 than the individual contributions would suggest.

We note here that the shape of the C_ℓ for the tensor (gravitational wave) modes is largely independent of Ω_0 (Turner, White & Lidsey 1993). For this reason the radiation power spectrum of a Λ model with some tilt and a component of tensors can exhibit less curvature at $\ell \sim 10$ than a purely scalar power spectrum (see Fig. 4). Since in some inflationary models we expect a non-negligible tensor component (Davis et al. 1992, but see Liddle & Lyth 1992, Kolb & Vadas 1993) we have computed the tensor C_ℓ following Crittenden et al. (1993) and give results both including and excluding a significant tensor contribution. Our results update those of Kofman, Gnedin & Bahcall (1993) who also considered tilted, Λ CDM models with a component of gravity waves.

In open models, where curvature domination occurs early, much of the large-angle anisotropy comes from the ISW effect (Hu & Sugiyama 1995) so the matter-to-radiation normalization is even more complicated. For open models the dependence of $P(k \rightarrow 0)/C_{10}$ on Ω_0 is not well fit by a power law, since the shape of the C_ℓ on all scales depends on Ω_0 . Fig. 6 shows the normalization on smaller scales for a model with $P(q)$ given by Eq. A3, where $q^2 = k^2/(-K) - 1$ and $K = H_0^2(\Omega_0 - 1)$. [The C_ℓ in this model will be similar to those in the inflationary models of Bucher et al. (1995) and Yamamoto et al. (1995). For a discussion of $P(q)$ in open models see the appendix.] Notice that, for fixed h and CMB normalization, the open models predict a smaller amplitude for the matter fluctuations today than the Λ models. We can understand this as a consequence of the earlier onset of curvature domination than Λ domination and the consequently stronger suppression of fluctuation growth in open models.

In Tables 1 and 2, and in Fig. 6, we show the normalization of the matter power spectrum for a range of models where the CMB normalization (C_{10}) is held fixed. We quote both the value of the RMS density fluctuation at $0.028 h \text{Mpc}^{-1}$ (large-scale) and σ_8 (small-scale). For comparison, Peacock & Dodds (1994) give

$$\Delta^2 (k = 0.028 h \text{Mpc}^{-1}) \equiv \frac{d\sigma_\rho^2}{d \ln k} = (0.0087 \pm 0.0023) \Omega_0^{-0.3}. \quad (18)$$

There are many determinations of σ_8 ; we quote here those from Peacock & Dodds (1994)

$$\sigma_8 = 0.75\Omega_0^{-0.15} \quad (19)$$

and cluster abundances (White, Efstathiou & Frenk 1993)

$$\sigma_8 = 0.57\Omega_0^{-0.56} \quad (20)$$

where the scaling with Ω_0 in both cases refers to models with $\Omega_0 + \Omega_\Lambda = 1$. These values are consistent with those inferred from large-scale flows (Dekel 1994) and direct observations (Loveday et al. 1992). In Fig. 7 we compare these observations with the COBE-normalized values of σ_8 for a range of Λ CDM models.

Conclusions

The COBE data forms a unique and valuable resource for the study of inhomogeneous cosmology. To fully exploit this hard won information we need to go beyond methods of normalizing theories of structure formation which use only gross properties of the data (such as the RMS fluctuation). In this paper we have presented a model independent method of parameterizing the COBE data, and discussed the normalization of the radiation and matter power spectra for a range of theoretically interesting models. In addition we considered the question of the goodness of fit of some commonly adopted models to the data from two complementary statistical standpoints.

Acknowledgments

We thank Douglas Scott for useful conversations and Joe Silk for suggesting we include a tensor contribution to the Λ models. We would also like to thank Ned Wright for comments on the manuscript and Section 3 in particular. The COBE data sets were developed by the NASA Goddard Space Flight Center under the guidance of the COBE Science Working Group and were provided by the NSSDC. This work was supported in part by grants from the NSF and DOE.

Appendix

In this appendix we make some comments about the fluctuation spectrum in an open universe. The material is taken from the work of Lyth & Stewart (1990), Ratra & Peebles (1994, and references therein), Bucher et al. (1995) and Lyth & Woszczyna (1995). These papers are sophisticated and rigorous treatments of the subject, and consequently are somewhat lengthy and technical in parts. Here we try to give a flavor of the problem, building on the rigorous results of those works. We will proceed in historical order.

We start by recalling a few points about inflationary cosmology. In an inflationary theory with $\Omega_0 = 1$, quantum fluctuations during inflation give rise to density and potential fluctuations today (see e.g. Olive 1990, Mukhanov et al. 1992, Kolb & Turner 1990, Linde 1990 and references therein). The amplitude of the fluctuations is set by the Hubble constant, H_{inf} , when the perturbation crosses out of the horizon, with larger scales (today) crossing the horizon earlier during inflation. If the potential of the inflaton (and hence H_{inf}) does not change very much during the time fluctuations on the relevant scales are produced (exponential inflation) one obtains a scale-invariant spectrum of fluctuations: $\delta^2 \propto k$. In terms of potential fluctuations, which are the perturbations which enter the underlying metric and are in some sense more fundamental than the density perturbations, this corresponds to $\delta\Phi = \text{constant} \propto H_{\text{inf}}/m_{\text{Pl}}$. (This spectrum is therefore described as scale invariant.) In Lyth & Stewart (1990) it was shown that, for scales which entered the horizon “early” when curvature could be neglected, $\delta\Phi = \text{constant}$ for $\Omega_0 < 1$ also. The transformation from this statement about the fluctuations in Φ per logarithmic interval to one about $P(k)$ proceeds in two steps. First, we relate the density perturbations to the potential fluctuations through Poisson’s equation, which in an open universe reads (Mukhanov et al. 1992)

$$(k^2 - 3K) \delta\Phi_k = 4\pi a^2 \rho \delta_k \quad (A1)$$

where the curvature scale is $K = H_0^2(\Omega_0 - 1)$ as before. Second, we note that in an open universe, the eigenfunctions of the operator ∇^2 with eigenvalues $k \geq \sqrt{-K}$ form a complete set (Lifshitz & Khalatnikov 1963, Harrison 1970, Abbott & Schaefer 1986). Thus we can expand all perturbations in term of these eigenfunctions. It is convenient to introduce the new variable $q^2 = k^2/(-K) - 1$ which runs from 0 to ∞ . [In order to obtain the most general gaussian random field in an open Universe, one must in general include the eigenfunctions with $0 \leq k \leq \sqrt{-K}$; however, for fluctuations generated by inflation only modes with $k \geq \sqrt{-K}$ are excited (Lyth & Woszczyna 1995)]. Recall it is $\delta\Phi_k^2 dk/k$ or $P(k)d^3k$ which gives the physical fluctuations, so we need to compare the power per logarithmic interval in k to the volume element in the two coordinates

$$4\pi \frac{dk}{k} = \frac{d^3k}{k^3} = \frac{d^3q}{q(q^2 + 1)}. \quad (A2)$$

Writing $k^2 - 3K \propto q^2 + 4$, and using the Poisson equation to translate from potential fluctuations (squared, per $\ln k$) to density fluctuations (squared, per d^3q) we have

$$P(q) \propto \frac{(q^2 + 4)^2}{q(q^2 + 1)} \quad (A3)$$

which is the result of Lyth & Stewart (1990). Ratra & Peebles (1994) performed a calculation of fluctuations from a linear potential in which they showed that this result extends to *all* q , not just those which entered the horizon while $\Omega \simeq 1$.

In a recent paper, Bucher et al. (1995) consider an explicit model for open universe inflation. [A similar calculation has been done by Yamamoto et al. (1995)]. In this model the inflaton first gets trapped in a false minimum of the potential for some time. During this time the universe inflates exponentially. The quantum fluctuations in the zero point energy are (power-law) suppressed by the existence of a mass gap (the inflaton has a mass, since the potential has curvature at the minimum $V(\varphi) = V_0 + m^2\varphi^2/2 + \dots$). The inflaton then tunnels through the barrier in the standard semi-classical way (c.f. nuclear decay) and nucleates a bubble of $\Omega_0 \simeq 0$ universe. As the potential rolls slowly from its post-tunneling value to the minimum of the potential more fluctuations are generated. The upshot of this, after a strenuous calculation, is that the potential fluctuations on small scales are $\delta\Phi = \text{constant}$, as before. On larger scales, corresponding to earlier times during inflation, the potential fluctuations are either enhanced or reduced, depending on the value of m in the potential. For the value of m considered in Bucher et al. (1995) one finds an enhancement by an extra factor of q^{-1} on very large scales. It is worthwhile to stress however that the C_ℓ are relatively insensitive to $q \lesssim 1$ within reasonable variations in $P(q)$.

The issue of fluctuations in open-universe inflation is not settled. Further theoretical work is required to determine whether inflation makes a unique prediction for the fluctuation spectrum in an open Universe, or whether we must rely on experiments to distinguish among the different possibilities. Should the power spectra rise as q^{-1} or q^{-2} on large scales, as currently predicted, then models with Ω_0 between 0.1 and 0.3 will be disfavored by the COBE data.

Tables

Ω_0	n	D'_1	D''_1	Δ^2	σ_8	D'_1	D''_1	Δ^2	σ_8
0.50	0.85	-0.079	0.476	0.027	1.45	-0.186	0.910	0.015	1.08
	0.90	0.046	0.503	0.031	1.62	-0.043	0.785	0.020	1.31
	0.95	0.172	0.557	0.036	1.82	0.115	0.693	0.028	1.62
	1.00	0.298	0.635	0.040	2.05	0.298	0.635	0.040	2.05
0.40	0.85	-0.110	0.600	0.030	1.29	-0.202	0.955	0.016	0.95
	0.90	0.012	0.631	0.034	1.45	-0.065	0.853	0.022	1.15
	0.95	0.135	0.685	0.039	1.62	0.084	0.787	0.030	1.43
	1.00	0.258	0.767	0.045	1.82	0.258	0.767	0.045	1.82
0.30	0.85	-0.159	0.853	0.032	1.10	-0.225	1.058	0.016	0.79
	0.90	-0.040	0.885	0.036	1.24	-0.097	0.991	0.022	0.97
	0.95	0.080	0.944	0.041	1.39	0.041	0.975	0.031	1.21
	1.00	0.201	1.022	0.047	1.56	0.201	1.022	0.047	1.56
0.20	0.85	-0.240	1.338	0.029	0.82	-0.258	1.237	0.014	0.56
	0.90	-0.124	1.366	0.033	0.92	-0.143	1.229	0.019	0.69
	0.95	-0.008	1.415	0.038	1.03	-0.023	1.295	0.027	0.88
	1.00	0.108	1.485	0.043	1.15	0.108	1.485	0.043	1.15
0.10	0.85	-0.342	2.455	0.014	0.33	-0.275	1.561	0.006	0.21
	0.90	-0.227	2.462	0.016	0.37	-0.176	1.673	0.008	0.26
	0.95	-0.113	2.485	0.019	0.41	-0.082	1.931	0.012	0.33
	1.00	0.000	2.527	0.022	0.46	0.000	2.527	0.022	0.46

Table 1: The shape of the radiation power spectrum in a Λ CDM model with $h = 0.75$. Also shown is the matter power spectrum normalization with the radiation normalized to $C_{10} = 10^{-11}$. For the tilted models we show the results with (right columns) and without (left columns) a gravity wave component with $C_2^T/C_2^S = 7(1 - n)$.

Ω_0	n	D'_1	D''_1	Δ^2	σ_8	D'_1	D''_1	Δ^2	σ_8
0.50	0.85	-0.001	0.657	0.018	0.80	-0.123	1.039	0.010	0.60
	0.90	0.130	0.698	0.020	0.89	0.028	0.937	0.013	0.72
	0.95	0.262	0.769	0.023	1.00	0.196	0.877	0.018	0.89
	1.00	0.396	0.866	0.026	1.12	0.396	0.866	0.026	1.12
0.40	0.85	-0.018	0.807	0.018	0.67	-0.130	1.099	0.010	0.50
	0.90	0.111	0.851	0.021	0.75	0.016	1.021	0.013	0.60
	0.95	0.240	0.924	0.024	0.84	0.178	0.992	0.019	0.74
	1.00	0.372	1.025	0.027	0.94	0.372	1.025	0.027	0.94
0.30	0.85	-0.043	1.104	0.017	0.51	-0.140	1.222	0.009	0.36
	0.90	0.084	1.154	0.020	0.56	-0.000	1.188	0.012	0.44
	0.95	0.212	1.227	0.022	0.63	0.155	1.212	0.017	0.55
	1.00	0.340	1.327	0.026	0.70	0.340	1.327	0.026	0.70
0.20	0.85	-0.071	1.668	0.013	0.32	-0.147	1.436	0.006	0.22
	0.90	0.055	1.719	0.015	0.35	-0.015	1.471	0.008	0.27
	0.95	0.180	1.788	0.017	0.39	0.131	1.594	0.012	0.34
	1.00	0.307	1.883	0.019	0.44	0.307	1.883	0.019	0.44
0.10	0.85	-0.029	2.910	0.003	0.13	-0.112	1.806	0.001	0.08
	0.90	0.096	2.946	0.004	0.14	0.018	1.978	0.002	0.10
	0.95	0.222	2.998	0.004	0.15	0.163	2.326	0.003	0.13
	1.00	0.347	3.072	0.005	0.17	0.347	3.072	0.005	0.17

Table 2: As in Table 1 but with $h = 0.50$.

Model	D'_1	D''_1	L	Consistency Probability
1	0.4	-1.6	3.29	78.0%
2	0	0	1.00	86.3%
3	-0.5	3.5	0.091	93.0%
4	-2	0	0.014	97.2%
5	-0.342	2.455	0.186	92.4%
6	-0.275	1.561	0.310	91.4%

Table 3: Bayesian and frequentist measures of goodness of fit for six cosmological models (see text). The shape parameters D'_1 and D''_1 are defined in the text. L denotes the Bayesian peak likelihood, normalized so that a pure Harrison-Zel'dovich Sachs-Wolfe model has $L = 1$. The consistency probability is the percentage of simulated data sets for which the goodness-of-fit parameter η defined in Eq. 14 is less than the value found for the real data.

Figure Captions

Fig. 1: The value of the RMS power, as measured by $\sigma(7^\circ)$ (solid) and $\sigma(10^\circ)$ (dashed), for the best fitting, tilted Sachs-Wolfe models, as a function of n . The fact that the RMS fluctuation of the best fitting model depends on n shows that there is more information in the COBE data than just the RMS power.

Fig. 2: The likelihood, L , as a function of the power spectrum shape parameters D'_1 and D''_1 . The contours range from $L = 0.5$ to $L = 3$ in steps of 0.5, where $L = 1$ corresponds to a flat spectrum $D'_1 = D''_1 = 0$. For values of (D'_1, D''_1) for which the power spectrum goes negative over the range $2 \leq \ell \leq 30$ (lower right corner) we have set the likelihood to zero.

Fig. 3: The data z_i (see Eq. 13) normalized to a Harrison-Zel'dovich spectrum (triangles) and our worst fitting model, model 4 of Table 3 (squares). The z_i shown were computed with a bin size $K = 20$. The solid and dashed lines show the expectation value of each z_i and approximate one-sigma deviations from it. (The z_i are only approximately χ^2 distributed and only approximately uncorrelated, so these estimated deviations are not precise.) The effective ℓ values probed by the different modes are indicated at the top of the figure. These quantities were computed by expanding each eigenmode f_j in spherical harmonics and computing the centroid of the distribution in ℓ -space, as described in the text. Note that with our definition the z_i only loosely correspond to C_ℓ and depend on the theory. At higher i the modes are sampling mostly noise and therefore change very little as the model parameters are changed.

Fig. 4: The power spectrum of fluctuations for a Λ CDM model with and without the tensor contribution. The models shown have $h = 0.75$, $\Omega_0 = 0.1$ and $n = 0.85, 0.90, 0.95$ (bottom to top). The solid lines are scalar only, while the dashed lines have $C_2^T/C_2^S = 7(1 - n)$. Note the tensor+scalar models have less curvature than the scalar only models, which makes them a better fitted to the COBE data.

Fig. 5: An example of how the normalization of the matter power spectrum depends on Ω_0 in a Λ CDM model (with $n = 1$). All quantities are normalized to their values at $\Omega_0 = 0.5$. The solid line is the RMS temperature fluctuation with C_{10} fixed. The dotted line shows the ratio of the large-scale matter normalization ($\lim_{k \rightarrow 0} P(k)/k$) to C_{10} . The dashed lines show the effect of the shift in matter-radiation equality on the small-scale normalization σ_8 , holding the large-scale normalization $\lim_{k \rightarrow 0} P(k)/k$ fixed. We show two models: $h = 0.75$ (upper) and $h = 0.50$ (lower) with $\Omega_B h^2 = 0.0125$.

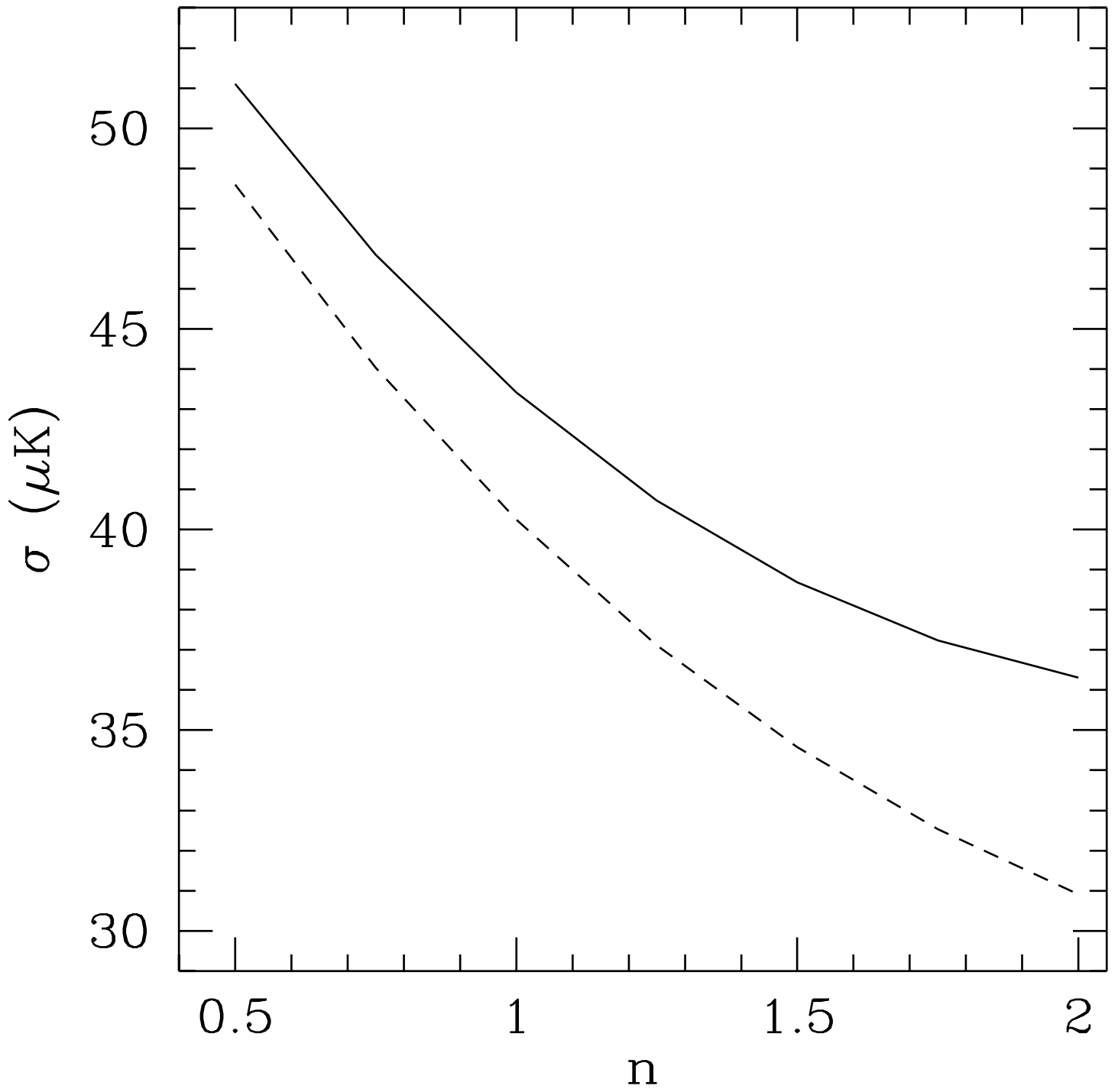
Fig. 6: The normalization, $\Delta^2(0.028h\text{Mpc}^{-1})$, as a function of Ω_0 for open CDM (dashed) and Λ CDM (solid) models normalized to $C_{10} = 10^{-11}$. In both cases the upper curves are for $h = 0.75$ and the lower curves are for $h = 0.50$, both with $\Omega_B h^2 = 0.0125$.

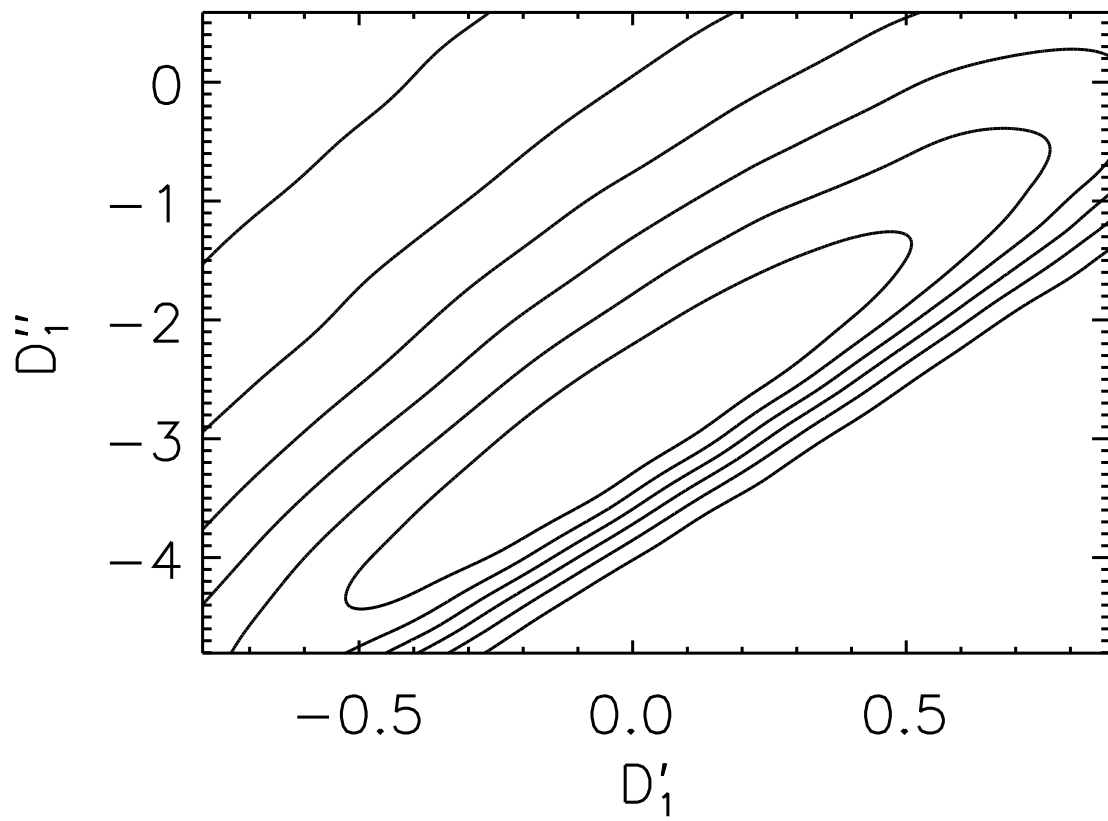
Fig. 7: The small scale normalization σ_8 vs Ω_0 in Λ CDM models, with normalization set by Eq. 9. The dashed lines assume all the contribution to the temperature fluctuations measured by COBE come from scalar perturbations; the dotted lines are scalars + tensors with $C_2^T/C_2^S = 7(1 - n)$. Slope (n) increases from 0.85 to 1.00 in steps of 0.05 with lowest n being lowest σ_8 . The two solid lines are two observational determinations of σ_8 , the top line from cluster abundances and the bottom line from large scale structure (i.e. Eqs. 19, 20).

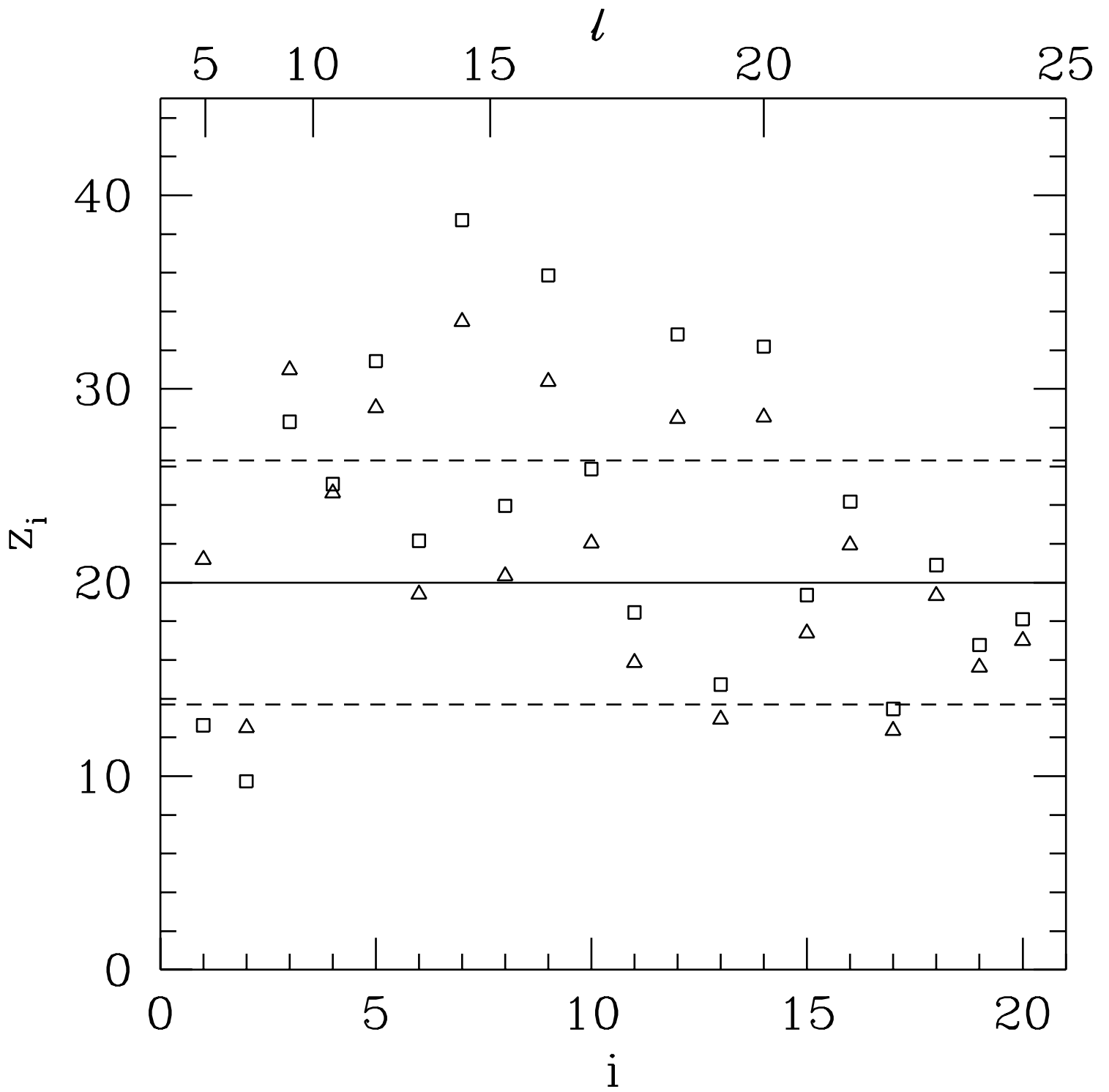
References

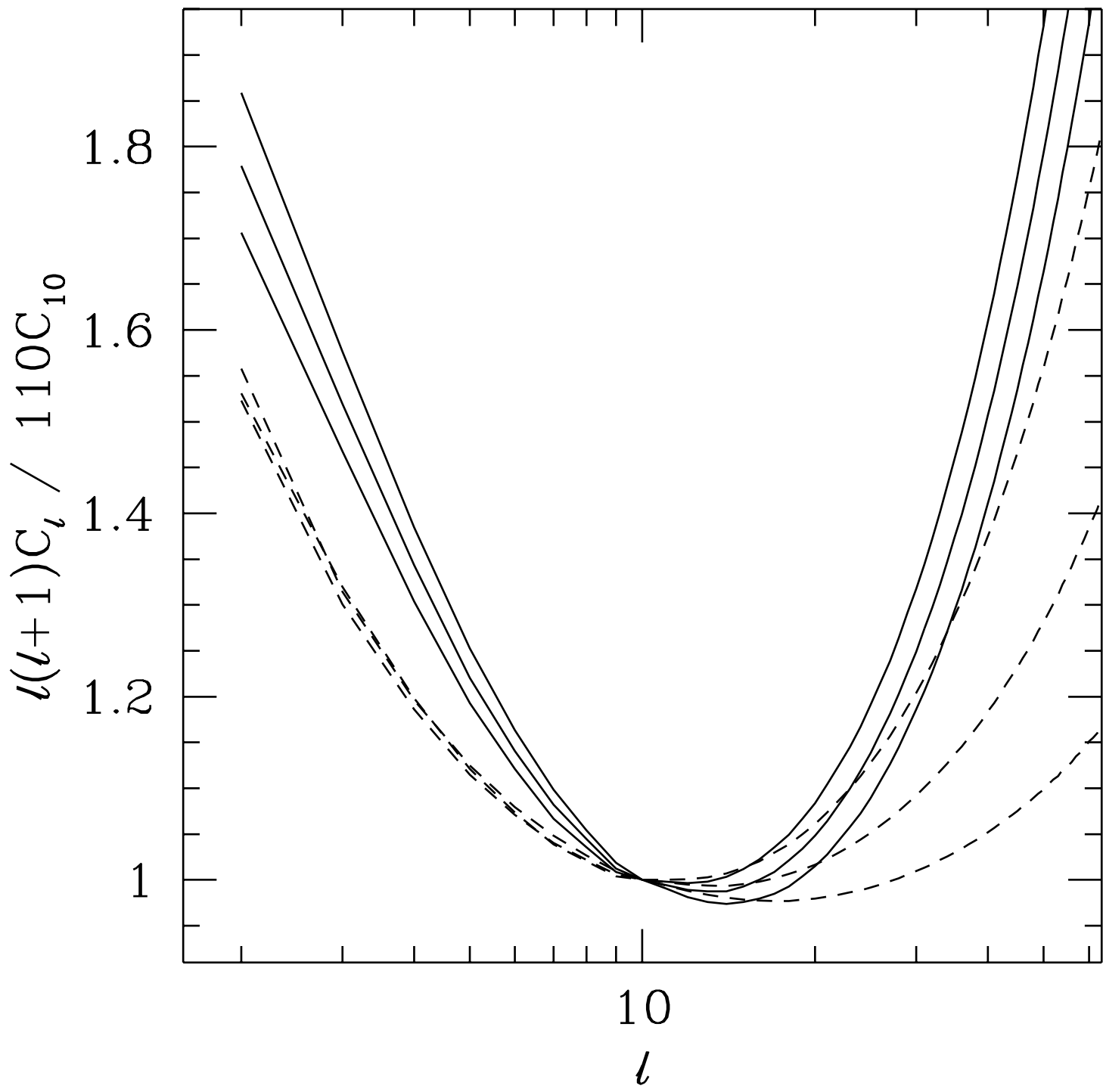
- Abbott, L. F., & Schaefer, R. K., 1986, *ApJ*, **308**, 546
- Banday, A.J. et al. 1994, *ApJ*, **436**, L99
- Bennett, C. L., et al. 1994, *ApJ*, **436**, 423
- Bucher, M., Goldhaber, A., & Turok, N., 1995, *Phys. Rev.*, in press
- Bunn, E., Scott, D., & White, M., 1995, *ApJ*, **441**, L9
- Bunn, E., & Sugiyama, N., 1995, *ApJ*, **446**, 49
- Carroll, S. M., Press, W. H., & Turner, E. L., 1992, *Ann. Rev. A. & Astrophys.*, **30**, 499
- Crittenden, R., Bond, J. R., Davis, R. L., Efstathiou, G., & Steinhardt, P. J., 1993, *Phys. Rev. Lett.*, **71**, 324
- Davis, R. L., Hodges, H. M., Smoot, G. F., Steinhardt, P. J., Turner, M. S., 1992, *Phys. Rev. Lett.*, **69**, 1856 (erratum: 70:1733)
- Efstathiou, G., Bond, J. R., & White, S. D. M., 1992, *MNRAS*, **258**, 1 p
- Górski, K. M., et al. 1994, *ApJ*, **430**, L89
- Górski, K. M., et al. 1995a, COBE, preprint
- Górski, K. M., et al. 1995b, in, preparation
- Hu, W. & Sugiyama, N. 1995, *ApJ*, **444**, 489
- Karhunen, K. 1947, *Über lineare Methoden in der Wahrscheinlichkeitsrechnung*, Helsinki: Kirjapaino oy. sana
- Kofman, L., Gnedin, N. Y., & Bahcall, N. A., 1993, *ApJ*, **413**, 1
- Kofman, L., & Starobinsky, A., 1985, *Sov. Astron. Lett.*, **11**, 271
- Kolb, E. W., & Vadas, S., 1993, *Phys. Rev.*, **D50**, 2479
- Kolb, E. W., & Turner, M. S., 1990, *The Early Universe*, Addison Wesley
- Harrison, E. R., 1970, *Phys. Rev.*, **D1**, 2726
- Liddle, A. R., & Lyth, D. H., 1992, *Phys. Lett.*, **B291**, 391
- Liddle, A. R., & Lyth, D. H., 1995, *MNRAS*, in press
- Lifshitz, E. M., & Khalatnikov, I. M., 1963, *Adv. Phys.*, **12**, 185
- Linde, A., 1990, *Particle Physics and Inflationary Cosmology*, Harwood Academic
- Lineweaver, C.H., Smoot, G.F., Bennett, C.L., Wright, E.L., Tenorio, L., Kogut, A., Keegstra, P.B., Hinshaw, G., & Banday, A.J., 1994, *ApJ*, **436**, 452
- Loveday, J. S., Efstathiou, G., Peterson, B. A. & Maddox, S. J., 1992, *ApJ*, **400**, L43
- Lyth, D. H. & Stewart, E., 1990, *Phys. Lett.*, **B252**, 336
- Lyth, D. H. & Woszczyna, A., 1995, Lancaster, preprint
- Mukhanov, V. F., Feldman, H. A., & Brandenberger, R. H., 1992, *Phys. Rep.*, **215**, 203
- Olive, K., 1990, *Phys. Rep.*, **190**, 307
- Peacock, J. A. & Dodds, S. J., 1994, *MNRAS*, **267**, 1020

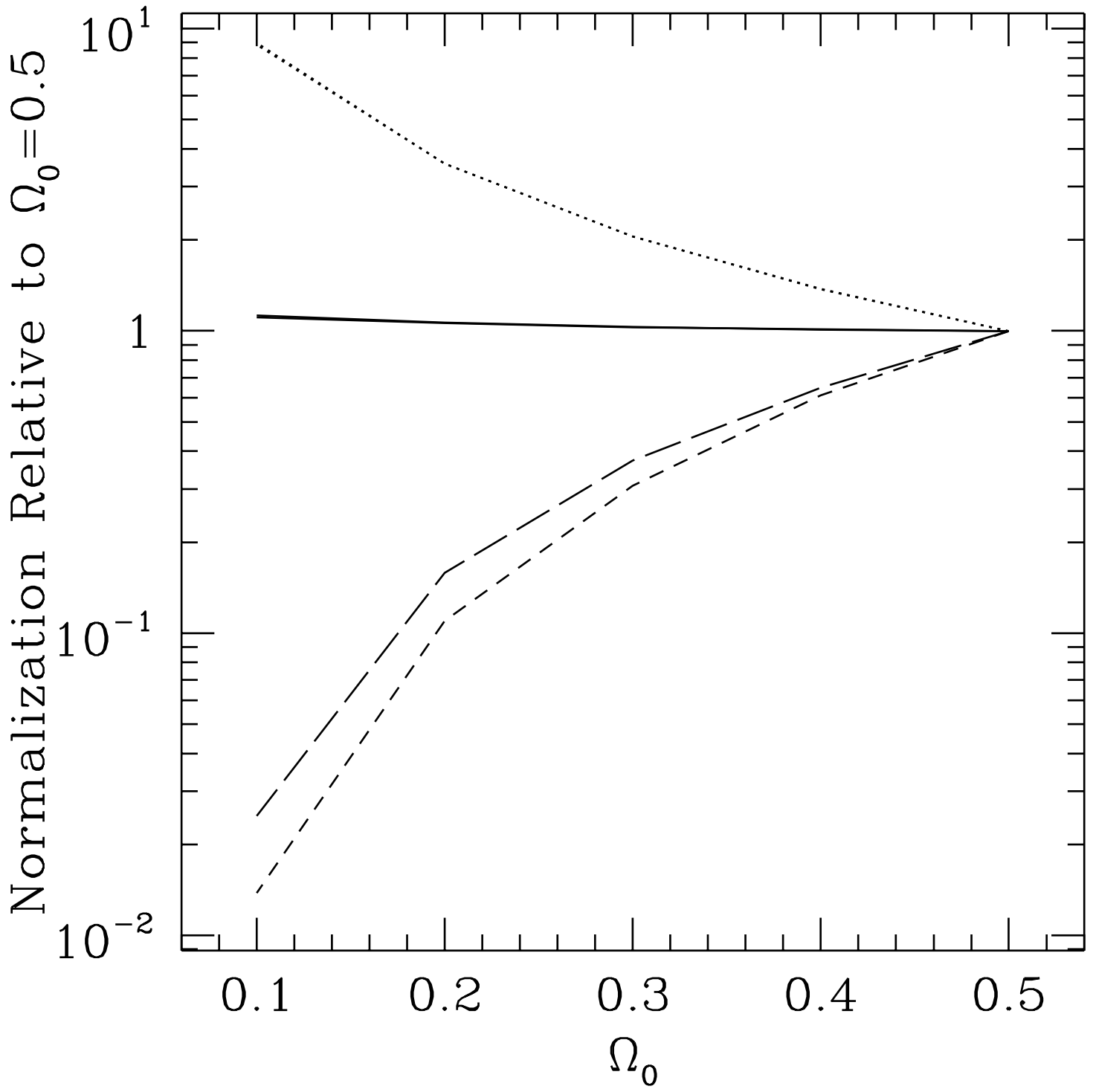
- Peebles, P. J. E., 1993, *Principles of Physical Cosmology*, Princeton UP
- Ratra, B., & Peebles, P. J. E., 1994, *ApJ*, **432**, L5
- Sachs, R. K., & Wolfe, A. M., 1967, *Ap. J.*, **147**, 73
- Smoot, G., et al., 1992, *ApJ*, **396**, L1
- Tegmark, M. & Bunn, E.F., 1995, Berkeley, preprint
- Thierren, C.W., 1992, *Discrete Random Signals and Statistical Signal Processing*, Prentice-Hall
- Turner, M. S., White, M., & Lidsey, J. E., 1993, *Phys. Rev.*, **D48**, 4613
- White, M., 1994, *Astron. & Astrophys.*, **290**, L1
- White, M., Scott, D., & Silk, J., 1994, *Ann. Rev. A. & Astrophys.*, **32**, 319
- White, S.D.M., Efstathiou, G., & Frenk C. 1993, *MNRAS*, **262**, 1023
- Wright, E. L., Smoot, G. F., Bennett, C. L., & Lubin, P. M., 1994, *ApJ*, **436**, 443
- Yamamoto, K., Sasaki, M., & Tanaka, T., 1995, Kyoto, preprint

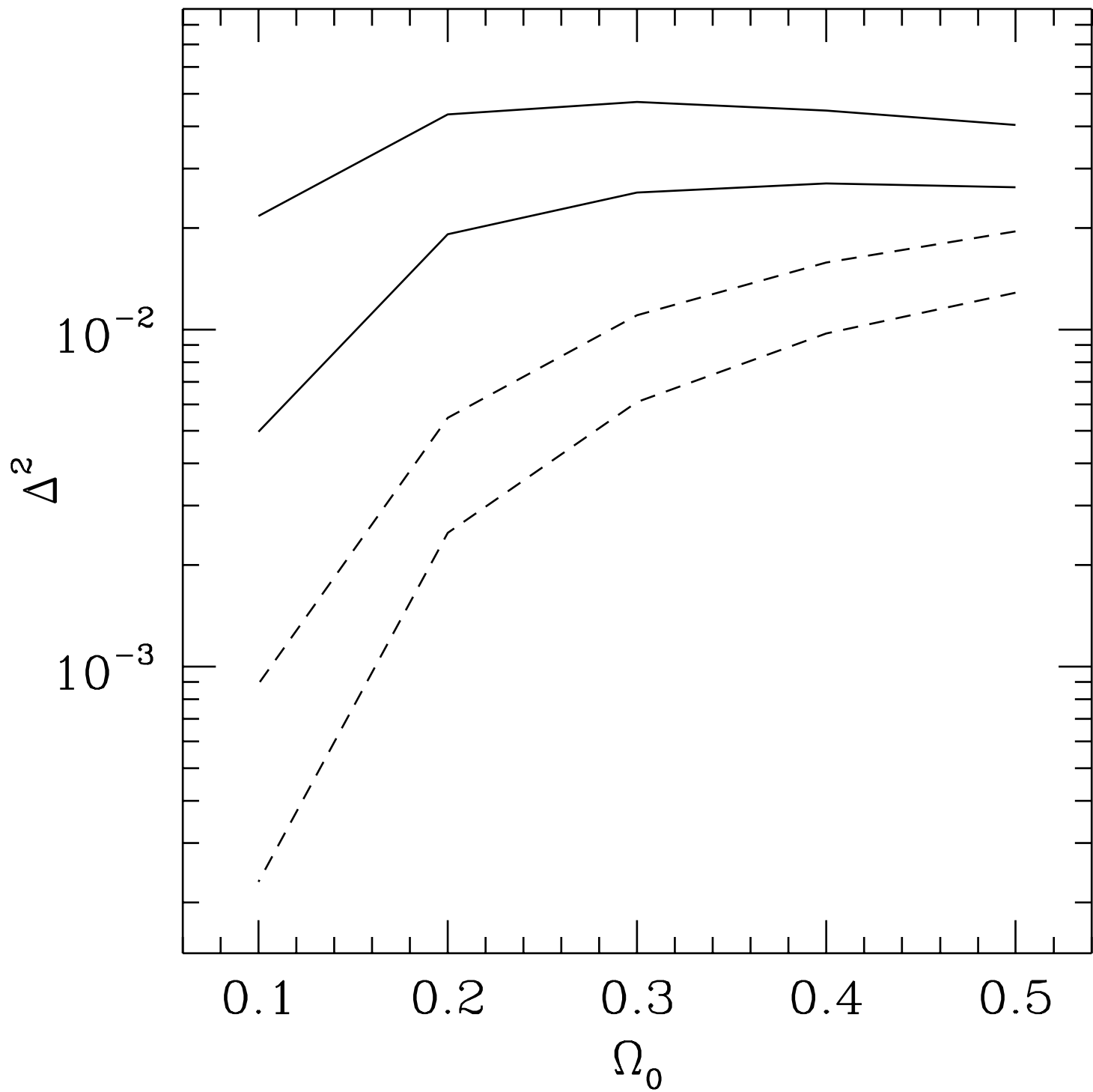


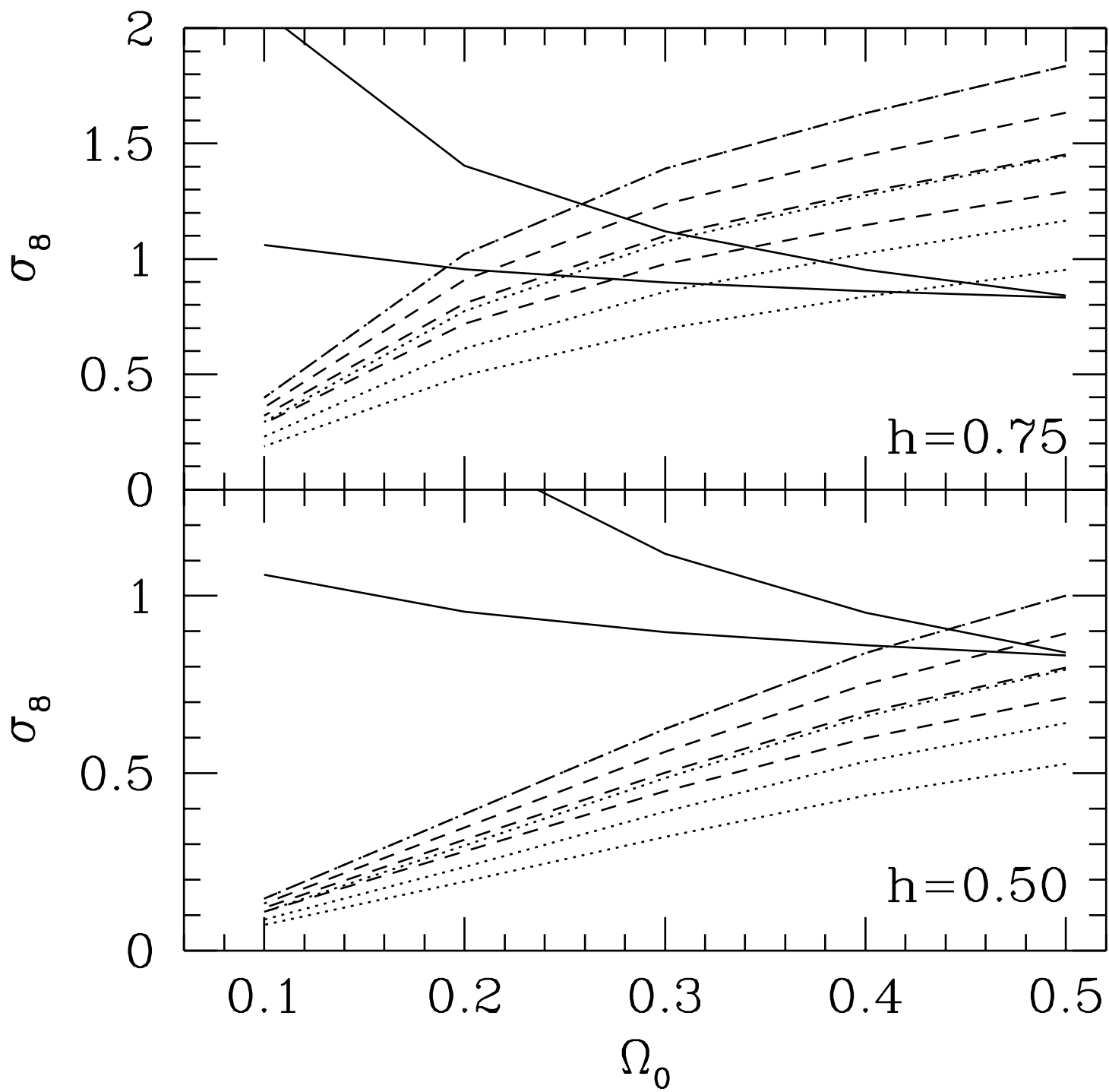












Erratum

The COBE Normalization of CMB Anisotropies

Martin White & Emory Bunn

Ap. J. **450**, 477 (1995)

In tables 1 & 2 the quoted values of Δ^2 and σ_8 assume a tensor-to-scalar ratio $C_2^T/C_2^S = 7(1-n)$. This is the correct lowest order (in an expansion in $1-n$) expression for the tensor-to-scalar ratio for $\Omega_0 = 1$. However the projection from the k -space inflationary prediction onto the quadrupole, i.e. $\ell = 2$ mode, has a dependence on Ω_Λ and n , which was neglected in calculating the entries in the tables. The “correction factor”, $f_{T/S}(\Omega_\Lambda, n)$, defined through

$$C_2^T/C_2^S = 7(1-n) f_{T/S}(\Omega_\Lambda, n)$$

can be well fit by

$$f_{T/S}(\Omega_\Lambda, n) = 0.97 - 0.58(1-n) + 0.25\Omega_\Lambda - [1 - 1.1(1-n) + 0.28(1-n)^2] \Omega_\Lambda^2 \quad .$$

This expression includes both the full n dependence (i.e. beyond leading order in $1-n$) of power-law inflation, for which exact expressions are available, and the ISW contribution to C_2^S . To good approximation the values of Δ^2 quoted in the tables should be multiplied by

$$\frac{1 + 7(1-n)}{1 + 7(1-n)f_{T/S}}$$

and the values of σ_8 by the square root of this. For reasonable values of Ω_Λ and n this amounts to a $\lesssim 10\%$ correction.